

## Corticotomy depth and regional acceleratory phenomenon intensity: A preliminary study

Jeremy R. Kernitsky<sup>a</sup>; Taisuke Ohira<sup>b</sup>; Dhurata Shosho<sup>c</sup>; June Lim<sup>d</sup>; Abdullah Bamashmous<sup>a</sup>; Serge Dibart<sup>e</sup>

### ABSTRACT

**Objectives:** To determine if the depth of corticotomy done with the piezoelectric knife could play a role in the intensity of the regional acceleratory phenomenon (RAP).

**Materials and Methods:** Eighteen Sprague-Dawley rats were divided into two groups: untreated (3 rats) and treatment (15 rats). In the treatment group, a split-model design was used. The right tibia received transcortical (deep) penetrations with the piezoelectric knife, while intracortical (shallow) penetrations were performed on the left tibia of the same animal. The rats were euthanized at day 1, 3, 7, 14, and 28. Cone-beam computed tomography scans were taken for each sample and then assessed by histological analysis.

**Results:** Higher amounts of osteoclastic activity and new collagen formation were observed in the deep penetration group when compared with the shallow penetration group. The former peaked at day 14 for both groups ( $1.53\% \pm 0.01\%$  vs  $0.03\% \pm 0.0004\%$ , respectively), and the latter peaked at day 28 ( $0.65 \times 10^6 \pm 0.01$  vs  $0.08 \times 10^6 \pm 0.0008$ , respectively).

**Conclusions:** Within the limitations of this study, it appears that the intensity of the RAP in the rat is corticotomy depth dependent. This is to be kept in mind when decorticating the bone during surgically facilitated orthodontic procedures. (*Angle Orthod.* 2021;91:206–212.)

**KEY WORDS:** Piezocision; Regional acceleratory phenomena; Corticotomy depth; Surgical facilitated orthodontics

### INTRODUCTION

The regional acceleratory phenomenon (RAP) is a concept introduced by Frost<sup>1</sup> that describes how an intentional surgical injury to the bone starts a cascade of physiologic events, leading to an increase in bone turnover with concomitant demineralization and new bone formation at the site of the bone injury.<sup>2,3</sup> This concept has been widely used to justify a variety of procedures involving surgically facilitated orthodontic treatments.<sup>4</sup> With the introduction of the piezoelectric knife into dentistry,<sup>5</sup> Dibart et al.<sup>4</sup> described a new approach, termed Piezocision<sup>TM</sup>. This technique is less invasive because it does not require the elevation of full-thickness flaps to perform the necessary alveolar decortications. Rather, decortications are done through interproximal buccal micro-incisions. This method is based on the judicious use of the RAP after bone injury with the piezoelectric knife to facilitate tooth movement. It is bimodal in nature with a demineralization phase and a remineralization phase.<sup>6</sup> This minimally invasive procedure also takes advantage of the unique properties of the piezoelectric knife and its vibration frequencies. In an earlier article, it was reported that

<sup>a</sup> Resident, Department of Periodontology, Boston University Henry M. Goldman School of Dental Medicine, Boston, Mass.

<sup>b</sup> Assistant Professor, Department of Periodontology, Boston University Henry M. Goldman School of Dental Medicine, Boston, Mass.

<sup>c</sup> Research Scientist, Department of General Dentistry, Division of Radiology, Boston University Henry M. Goldman School of Dental Medicine, Boston, Mass.

<sup>d</sup> Research Assistant, Department of Periodontology, Boston University Henry M. Goldman School of Dental Medicine, Boston, Mass.

<sup>e</sup> Professor and Department Chair, Department of Periodontology, Boston University Henry M. Goldman School of Dental Medicine, Boston, Mass.

Corresponding author: Dr Serge Dibart, Department of Periodontology, Boston University Henry M. Goldman School of Dental Medicine, 635 Albany Street, Second Floor, Boston, MA, 02118  
(e-mail: Sdibart@bu.edu)

Accepted: August 2020. Submitted: April 2020.

Published Online: November 11, 2020

© 2021 by The EH Angle Education and Research Foundation, Inc.

Piezotome 2–driven corticotomy generated, for the same surgical insult, a much greater degree of demineralization and remineralization when compared with bur- or screw perforation–type corticotomies in calvarial bone.<sup>7</sup> The next query was, How does the depth of bony penetration affect the RAP? Dibart<sup>8</sup> emphasized the need for a corticotomy that is deep enough to reach the medullary space to obtain a maximum RAP effect. The aim of the present study was to determine the veracity of that statement by comparing the effect of two different depth penetrations—intracortical (shallow) and transcortical (deep)—performed with the piezoelectric knife on the tibiae of young rats.

## MATERIALS AND METHODS

This study was approved by the Boston University Medical Center Institutional Animal Care and Use.

Animals were received from Charles River (Cambridge, Mass) and acclimatized in the Animal Science Center for 48 hours. Eighteen Sprague-Dawley male rats (age 9–10 weeks; weight 300–350 mg) were divided into two groups: untreated and treatment. The untreated group consisted of three animals that were sacrificed at baseline (day 0). The treatment group contained 15 animals. A split-model design was used in the treatment group. The right tibia of the rat received a transcortical penetration with the piezoelectric knife (Piezotome 2, Satelec, Acteon Group, France), while intracortical penetrations were performed on the left tibia. The rats (three in each time group) were euthanized with CO<sub>2</sub> asphyxia at five different postoperative timelines on days 1, 3, 7, 14, and 28.

### Surgical Procedure

The animals were fed rat chow and water ad libitum and weighed daily. For the surgical intervention, rats were anesthetized with intraperitoneally administered ketamine (75–95 mg/kg) and xylazine (5 mg/kg) in one bolus injection (Henry Schein, Melville, NY). The mesial surface of the rats' legs was shaved, and the exposed skin disinfected with three rounds of Betadine solution (povidone–iodine 5%, Avrio Health L.P., New York, NY) by scrubbing the shaved skin and further wiped with 70% isopropyl alcohol to remove the excess solution in the surgical area.

A longitudinal incision of approximately 1 cm was performed 6 mm below the knee on the medial side of the tibia. The medial side of the tibia diaphysis was exposed with a full-thickness flap, and corticotomy was performed using the BS1 insert 8 mm below the knee, with D1 settings. On the right side, a transcortical penetration was performed to reach the medullary

spaces (approximately 1-mm depth). Penetration through the cortical layer was confirmed by visual observation of bleeding from the surgical bony defect as well as manually with a dental explorer. On the left side, the intracortical penetration was performed with the Piezotome, lightly denting the tibial cortex but not going through it (approximately 0.5-mm depth). No bleeding from the surgical bony defect was observed, ensuring shallow decortication.

The surgical sites were then sutured with 5-0 Vicryl absorbable sutures (ACE Surgical Supply Co Inc, Brockton, Mass) to achieve primary closure, and a cone-beam computed tomography (CBCT) image was taken to confirm the corticotomy depth.

### Sample Collection

All animals survived and were sacrificed at the required time points. After the animals were euthanized, a small incision was made on the skin 1 cm over the knee, followed by careful dissection of the skin. The femur was disarticulated, and the entire leg (femur, knee, and tibia) was fixed with 4% paraformaldehyde for 48 hours at 4°C and then dehydrated in a 70% isopropyl alcohol solution. The soft tissues surrounding the tibia and knee were kept intact.

### CBCT

CBCT scans were taken for each sample and at all time intervals using the I-Cat Next Generation scanner (I-Cat, Hatfield, Penn). The samples were analyzed using In Vivo 6 software (Anatomage, Santa Clara, Calif). The sagittal cuts going through the center of the defects along the long axis of the tibia were recorded. This step was used to confirm the depth of penetration.

### Histology Processing

The labeled samples were placed in a decalcification solution (107.88 g of EDTA Na<sub>2</sub>\*2H<sub>2</sub>O and 0.8 g of NaOH in water, pH = 5.0) for 10 days until the tissues softened. The tissues were then dehydrated with increased concentrations of ethanol baths reaching 100% after 14.5 hours and submerged afterward in xylene. The samples were then embedded in paraffin. The blocks were sectioned longitudinally along the long axis of the tibia, and the samples were stained with hematoxylin and eosin (H&E), Accustain trichrome stain (Masson's), and tartrate-resistant alkaline phosphatase (TRAP).

### Data Analysis

All of the stained slides were scanned using a whole-field digital scanner (Panoramic MIDI, 3D Histech Ltd, Budapest, Hungary), allowing for analysis with Case

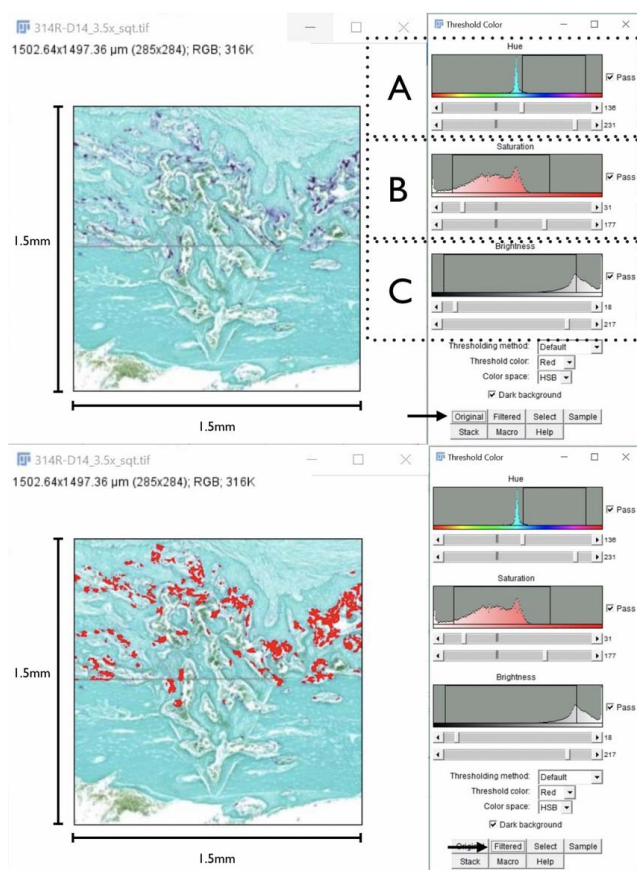


**Figure 1.** Method for threshold color measurements (Image J Software) used on the right: (A) adjustment of the filter by hue value, (B) adjustment of the filter by saturation value, (C) adjustment of the filter by brightness. Red shows the filtered areas. It is now possible to calculate the amount of osteoclast activity (red) in the specific area.

Viewer software (version 2.2, 3DHistech Ltd). The histological samples stained with TRAP were further analyzed using Image J software (version 1.8.0\_172, National Institutes of Health, Bethesda, Md) with the purpose of calculating the area of osteoclast activity (purple color) in a specific area ( $1.5 \times 1.5$  mm). The images in JPG format were opened with Image J software, and the threshold color analysis tool was used (Figure 1). This tool allowed for the selection of specific areas in an image filtered by pixel color (Figure 1). Once filtered, the measurement tool was used to calculate the area filled with red in the overall known area of the sample. A similar analysis was performed for the samples stained with Masson's stain, in which the color blue, which represents the presence of collagen, was filtered, and the area was calculated as described above.

### Statistical Analysis

For the statistical analysis, we used JMP Pro 14 software (SAS Institute Inc, Buckinghamshire, UK).

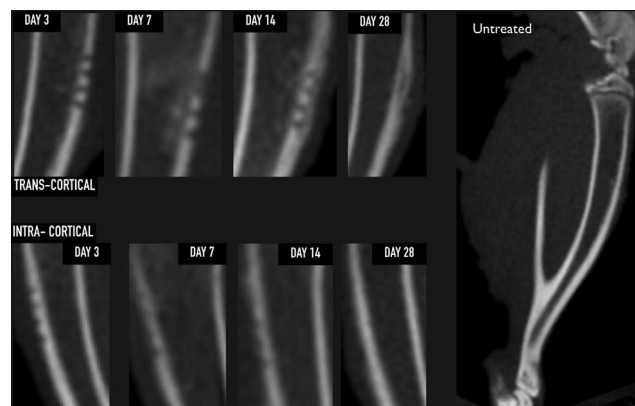


**Figure 2.** Sagittal cone-beam computed tomography section confirming proper corticotomy depth and the evolution of both treatment groups. Only the transcortical group reached the medullary space, showing an increase in radiopacity inside the medullary space by day 7 (callus formation) that completely disappeared by day 28. Day 28 shows new radio-opaque tissue located on the outer surface, suggesting an increase of the overall thickness of the cortical layer at the site of injury. None of these findings were observed in the intracortical group, in which, by day 28, there was radiographically no difference when compared with the untreated group.

Analysis of variance was used with a power of 95%. Statistical differences were considered significant at the 5% critical level. This was calculated only for the comparison of osteoclastic activity and new collagen formation over time.

## RESULTS

### CBCT

The tibia from the untreated sample showed an even and continuous radiopaque cortical layer of approximately 0.8- to 1.1-mm thickness in the sagittal cut, with a radiolucent medullary space present between the two cortical layers. The treatment group samples showed proper penetration depth, with the right tibia showing transcortical penetration and the left tibia intracortical penetration only (Figure 2).

### Histology

*Day 1 and 3.* On day 1, the intracortical penetration showed an injury contained within the cortical bone. The transcortical injury showed marrow penetration and subsequent formation of a blood clot in the marrow cavity (Figure 3). On day 1 in the intracortical site, the defect was occupied mostly by erythrocytes, with less than 5% of leukocytes. In the transcortical penetration sites, approximately 50% of erythrocytes were embedded in a fibrin mesh, the rest being leukocytes. These results suggested that most leukocytes present may have been coming from the marrow spaces instead of the periosteum. On day 3 in the intracortical site, the



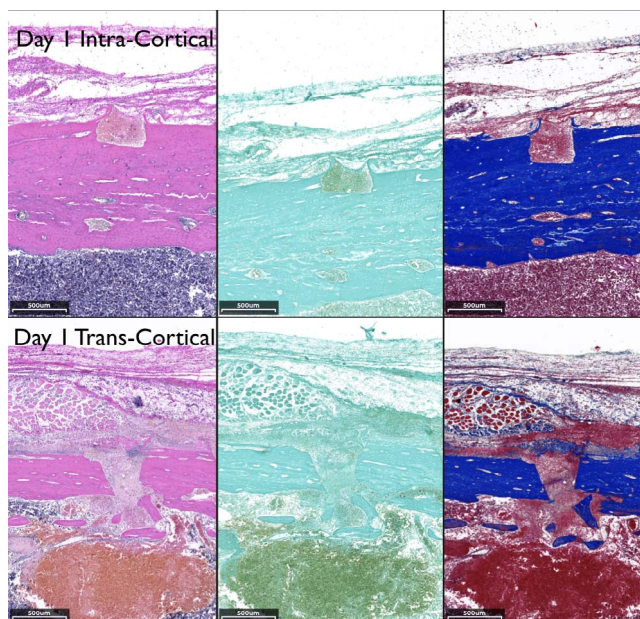


**Figure 3.** Histological comparison of the transcortical and intracortical penetration sites at day 1 using hematoxylin and eosin, tartrate-resistant alkaline phosphatase, and Masson's stains (left to right, 3.5× magnification).

erythrocytes were still occupying the center of the defect, and the presence of fibroblasts horizontally bridging the coronal portion of the defect was observed. In the transcortical site, the center of the defect was occupied by fibroblasts extending vertically from the marrow to the outer surface with erythrocytes present (Figure 4). There was undetectable osteoclastic activity at this time (Figure 3). Histological observation suggested an ongoing apoptotic process of osteocytes between day 1 and 3 (Figure 4).<sup>6</sup>

**Day 7 (resorption phase).** Significant changes were seen by day 7. The intracortical penetration group showed deposition of new collagen that almost entirely filled the defects, whereas the transcortical penetration group displayed a much more extensive response, especially in the medullary space, with new collagen making up an internal callus structure stained blue by the Masson's stain (Figure 5A). There was significant osteoclastic activity present, as illustrated by the TRAP staining in the callus as well as the endosteum side of the defect. In contrast, the intracortical penetration sites presented minimal to nonnoticeable osteoclastic activity.

**Day 14 (reversal and early formation phase).** At this time point, it was no longer possible to distinguish the defect areas in the intracortical group. In the transcortical penetration group, the intramedullary callus structure was almost completely resorbed, and the external callus was seen over the defect (Masson's stain). An important amount of osteoclastic activity was

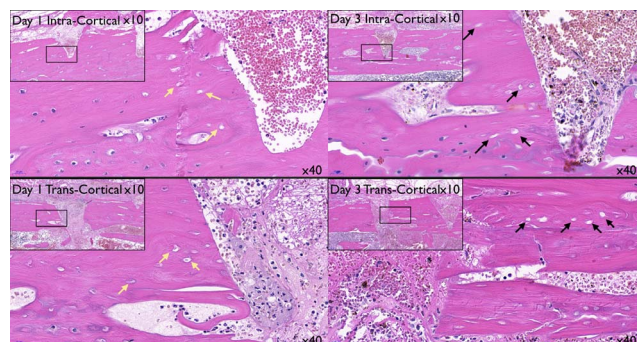


**Figure 4.** Histological comparison on days 1 and 3 from both treatment groups, suggesting osteocyte apoptosis. Day 1, the osteocytes nuclei are "shrunk" but still present in the lacunae for both groups (yellow arrows). Day 3, the osteocytes surrounding the defect area have lost their nuclei (black arrows), suggesting an ongoing apoptotic effect.

present in both the internal and outer layers of the cortical bone (Figure 5B).

**Day 28 (remodeling phase).** By day 28, the defects had healed in both groups; the transcortical penetration group showed that the internal callus had resorbed, while the external callus was present. There was an overall increased width of cortical bone due to the deposition of new bone on the outer surface. There was some limited osteoclastic activity in the newly formed bone (Figure 5C).

### Osteoclastic Activity

A higher amount of osteoclastic activity was observed in the transcortical (deep) penetration group as compared with the intracortical (shallow) penetration group (Figure 6). This activity increased at day 7 (transcortical  $1.352\% \pm 0.005\%$  vs intracortical  $0.001\%$ ) and seemed to peak at day 14 in both groups, with the transcortical penetration group showing a significant increase compared with the intracortical group ( $1.53\% \pm 0.01\%$  vs  $0.03\% \pm 0.0004\%$ , respectively). This osteoclastic activity decreased by day 28 ( $0.555\% \pm 0.002\%$  vs  $0.001\%$ , respectively).

### Collagen Formation

After analyzing the Masson's stain samples, the amount of new collagen formation (type 1) was calculated. New collagen formation in the intracortical penetration group remained the same throughout time and began to be detectable at day 7 and remained so until day 28. Significant changes could be observed in the transcortical penetration group (Figure 6), with significant increases in new collagen formation as compared with the intracortical group at day 7 ( $0.50 \times 10^6 \pm 0.004$  vs  $0.10 \times 10^6 \pm 0.001$ ) and day 28 ( $0.65 \times$

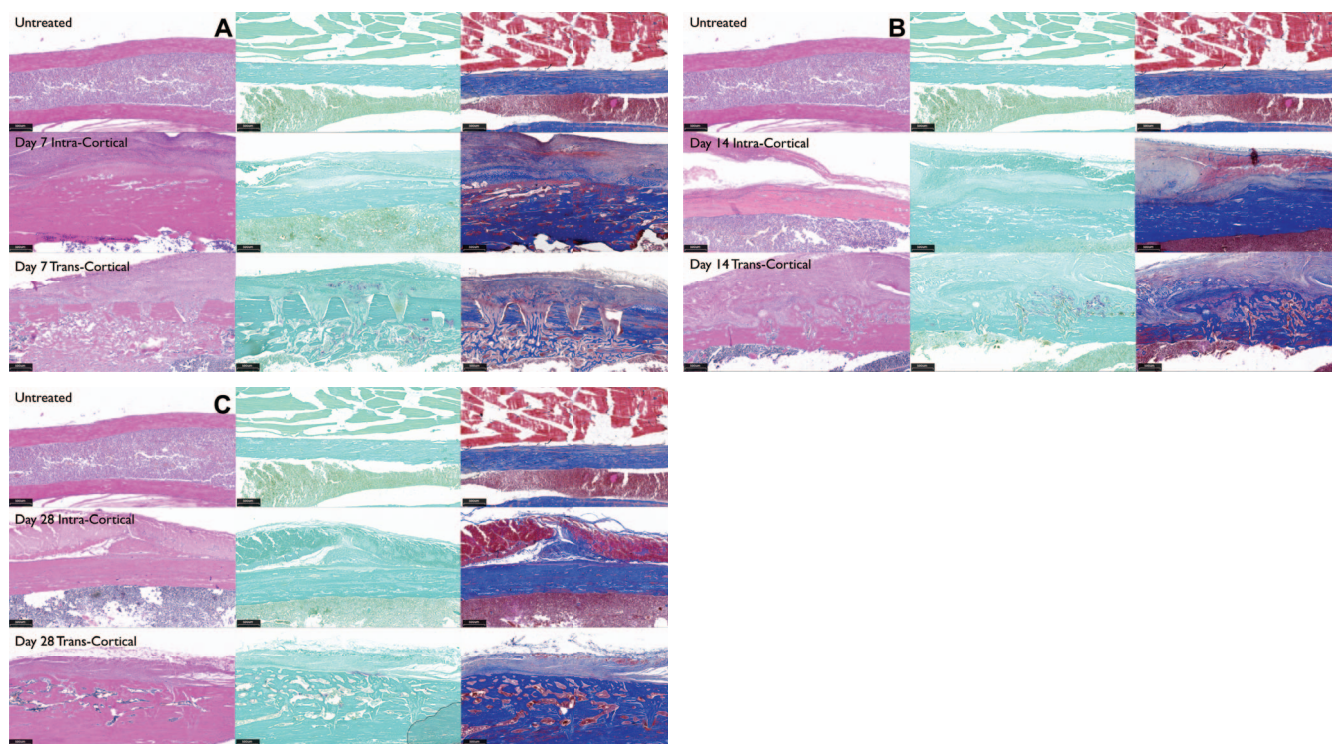


**Figure 5.** (A, B, C) Histological comparison of the untreated and treatment sites at days 7, 14, and 28 using hematoxylin and eosin, tartrate-resistant alkaline phosphatase, and Masson's stains (left to right, 3.5× magnification). (A) Day 7: the defects in the intracortical group were identified only with Masson's staining, where the defects are seen as red shadows in the middle of the blue stain. In the transcortical group, the defects reach the marrow spaces, and there is a formation of an internal callus; important TRAP activity can be seen. (B) Day 14: in the intracortical penetration group, the defects have completely healed. In the deep site, the internal callus has resorbed, the external callus is more noticeable, and there is significant osteoclastic activity in the area. (C) Day 28: the transcortical sites have a thickening of the bony cortex (Masson's stain) and limited osteoclastic activity.

$10^6 \pm 0.01$  vs  $0.08 \times 10^6 \pm 0.0008$ ). The "dip" seen at day 14 ( $0.21 \times 10^6 \pm 0.0048$  vs  $0.08 \times 10^6 \pm 0.0005$ ) reflected the resorption of the inner callus structure that had formed in the medullary space by day 7 and the restoration of the medullary cavity to its normal shape. The outer (periosteum) layer showed a gradual increase

of new collagen with bonelike structure at day 28, increasing the thickness of the tibial bone cortex.

## DISCUSSION

The results of this study may improve the understanding of how corticotomy depth can affect the extent

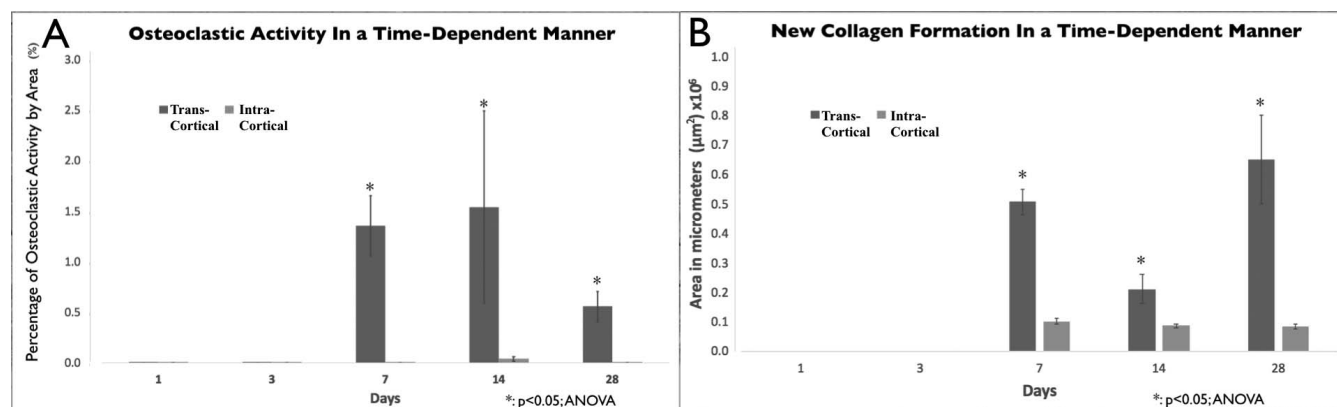


**Figure 6.** Osteoclastic activity and new collagen formation data. (A) Percentage of osteoclastic activity per day and depth of cortical penetration (tartrate-resistant alkaline phosphatase staining). (B) Mean area of new collagen formation by day and depth of cortical penetration (Masson's staining).



of the RAP. The study was conducted on a rat model. Rats share similarities and differences with humans.<sup>9</sup>

The basic metabolic rate in rats is ~6.4 times faster than that of humans.<sup>10</sup> As the rate of turnover and maturation is faster in rats, it allows us to observe the cycle of biological phenomenon (such as the RAP following injury) in a shorter period of time.

As Frost et al.<sup>1</sup> initially described, the more extensive the injury, the more intensive the response. The present study seems to validate this statement, as two very distinct responses were observed following intracortical and transcortical bone penetrations.

When the penetration extends and reaches the medullary space, the response seems to be greatly amplified. Similarly to what Mueller et al.<sup>11</sup> described, the inner callus formed at day 7 in the transcortical group was followed by an intense osteoclastic activity, resulting in the restoration of the medullary cavity to its normal anatomical shape.<sup>2</sup> In addition, new bone formed externally (periosteum side) by day 14 and increased the thickness of the cortical layer by 60% by day 28. A similar result was observed by Mueller et al.,<sup>11</sup> who described a 20% increase in new bone in the periosteum side after penetrations were performed with a surgical bur. Interestingly, when the corticotomy does not reach the medullary space, a significantly reduced tissue response is to be expected, in terms of both resorption and formation. A limited surgical injury (intracortical) will induce a moderate RAP, resulting in a limited amount of osteoclastic activity and bone turnover. This in turn may affect the rate and speed of tooth movement following any surgically facilitated orthodontic procedure that stays intracortical. This is critical to emphasize, because there have been some inconsistencies in the literature regarding the rate of tooth movement after Piezocision or some other surgically facilitated orthodontic procedures.<sup>12,13</sup> These conflicting results could be due to the differences in penetration depth during decortication procedures. A transcortical surgical penetration that reaches the alveolar bone marrow would lead to a powerful RAP that would maximize the speed of tooth movement when combined with orthodontics. Therefore, it would appear that the intensity and magnitude of the RAP could be depth dependent.

An apoptotic effect seemed to occur 72 hours after the surgical insult with the piezoelectric knife, suggesting the lack of nuclei present. This finding, germane to the piezoelectric knife at a specific frequency, was previously reported by Ohira et al.<sup>6</sup> and may be important for two reasons. First, the low-frequency vibrations generated by this piezoelectric technology do not seem to cause direct injury to the cells and induce necrosis. As described by Hollstein et al.<sup>14</sup> following the use of piezoelectric knife, the vitality of

osteocytes is preserved immediately after the osteotomy at sites adjacent to the defect area. This was seen in the present study, in which the vitality of the osteocytes seemed to be somewhat preserved until day 3, when signs of osteocyte death (apoptosis) were seen, possibly caused by the damaged osteocytes canaliculi.<sup>15</sup> Second, as described by Nakahama,<sup>16</sup> osteocyte apoptosis is considered to be a powerful promoter of osteoclastogenesis, initiating the bone-remodeling process due to an increase of cAMP levels on osteoblasts, triggering an increase in the formation of receptor activator of nuclear factor kappa-B ligand (RANKL) and reducing that of osteoprotegerin.

Another difference that could be observed within the treatment groups is the provenance of the cells in charge of bone formation. In the intracortical group, the cells are expected to come directly from the periosteum and potentially from the circulating blood and blood vessel pericytes.<sup>17</sup> These samples were completely healed by day 14 with no additional new bone formation. On the other hand, in the transcortical penetrations, the sources of cell provenance also included the endosteum and the medullary space. The latter is known to be a direct source of mesenchymal stem cells<sup>18</sup>; therefore, a more significant response could be anticipated (new bone formation).

The present study does have a number of limitations, such as the relatively small number of animals, making this a preliminary study. In addition, long bones were used instead of facial bones (chondrogenic vs intramembranous ossification), and micro-CT analysis was not performed. We also did not evaluate specific biomolecular signaling pathways, nor were we able to distinguish distinctly the source of the osteogenic cells, both of which would be important to clarify in future investigations.

## CONCLUSIONS

- Within the limitations of this study, it appears that the intensity of the RAP in the rat is corticotomy depth dependent.
- Following a deep penetration passing the cortex and reaching the medullary space with the piezoelectric knife, the RAP is more intense, generating a higher level of osteoclastic activity and bone turnover than a shallow injury. This leads to more extensive bone demineralization and may have unique clinical applications in terms of speed of tooth movement when combined with orthodontics.
- This is to be kept in mind when decorticating the bone during surgically facilitated orthodontic procedures.

## REFERENCES

1. Frost HM. The regional acceleratory phenomenon: a review. *Henry Ford Hosp Med J*. 1983;31:3–9.
2. Frost HM. The biology of fracture healing: an overview for clinicians. Part I. *Clin Orthop Relat Res*. 1989;(248):283–293.
3. Frost HM. The biology of fracture healing: an overview for clinicians. Part II. *Clin Orthop Relat Res*. 1989;(248):294–309.
4. Dibart S, Sebaoun JD, Surmenian J. Piezocision: a minimally invasive, periodontally accelerated orthodontic tooth movement procedure. *Compend Contin Educ Dent*. 2009;30:342–344, 346, 348–350.
5. Vercellotti T. Piezoelectric surgery in implantology: a case report—a new piezoelectric ridge expansion technique. *Int J Periodontics Restorative Dent*. 2000;20:358–365.
6. Ohira T, De Vit A, Dibart S. Strategic use of ultrasonic frequencies for targeted bone bio-modification following piezoelectric bone surgery in rats (part I: early phase). *Int J Periodontics Restorative Dent*. 2019;39:709–718.
7. Dibart S, Alasmari A, Zanni O, Salih E. Effect of corticotomies with different instruments on cranial bone biology using an ex vivo calvarial bone organ culture model system. *Int J Periodontics Restorative Dent*. 2016;36(suppl):s123–s136.
8. Dibart S. Piezocision™: accelerating orthodontic tooth movement while correcting hard and soft tissue deficiencies. *Front Oral Biol*. 2016;18:102–108.
9. Andreollo NA, dos Santos EF, Araújo MR, Lopes LR. Rat's age versus human's age: what is the relationship? *Arq Bras Cir Dig ABCD Braz Arch Dig Surg*. 2012;25:49–51.
10. Agoston DV. How to translate time? The temporal aspect of human and rodent biology. *Front Neurol*. 2017;8:92.
11. Mueller M, Schilling T, Minne HW, Ziegler R. A systemic acceleratory phenomenon (SAP) accompanies the regional acceleratory phenomenon (RAP) during healing of a bone defect in the rat. *J Bone Miner Res Off J Am Soc Bone Miner Res*. 1991;6:401–410.
12. Uribe F, Davoody L, Mehr R, et al. Efficiency of piezotome-corticision assisted orthodontics in alleviating mandibular anterior crowding: a randomized clinical trial. *Eur J Orthod*. 2017;39:595–600.
13. Librizzi Z, Kalajzic Z, Camacho D, Yadav S, Nanda R, Uribe F. Comparison of the effects of three surgical techniques on the rate of orthodontic tooth movement in a rat model. *Angle Orthod*. 2017;87:717–724.
14. Hollstein S, Hoffmann E, Vogel J, Heyroth F, Prochnow N, Maurer P. Micromorphometrical analyses of five different ultrasonic osteotomy devices at the rabbit skull. *Clin Oral Implants Res*. 2012;23:713–718.
15. Noble BS, Reeve J. Osteocyte function, osteocyte death and bone fracture resistance. *Mol Cell Endocrinol*. 2000;159:7–13.
16. Nakahama K-I. Cellular communications in bone homeostasis and repair. *Cell Mol Life Sci*. 2010;67:4001–4009.
17. Crisan M, Yap S, Casteilla L, et al. A perivascular origin for mesenchymal stem cells in multiple human organs. *Cell Stem Cell*. 2008;3:301–313.
18. Kobolak J, Dinnyes A, Memic A, Khademhosseini A, Mobasheri A. Mesenchymal stem cells: Identification, phenotypic characterization, biological properties and potential for regenerative medicine through biomaterial micro-engineering of their niche. *Methods*. 2016;99:62–68.